World Journal of Advanced Research and Reviews
eISSN: 2581-9615 CODEN (USA): WJARAI
Cross Ref DOI: 10.30574/wjarr
Journal homepage: https://wjarr.com/

(RESEARCH ARTICLE)

Check for updates

Opto-electronic properties of organic-inorganic Tin-based perovskite: A theoretical investigations

Mehtab-Ur-Rehman [1,*], Wang Qun [1], Yasar Ali [2], Fazal dayan [2], Waqas khan [2], Muhammad Murtaza [2] and AL-GALAL HASAN MUNASSAR SALEH [2]

[1] *Faculty of Materials and Manufacturing, Beijing University of technology, No.100, Pingleyuan, Chaoyang District, Beijing, China.*
[2] *MRS Institute of Physics and Mathematics, Pakistan.*

World Journal of Advanced Research and Reviews, 2023, 17(01), 836–845

Publication history: Received on 05 December 2022; revised on 20 January 2023; accepted on 23 January 2023

Article DOI: https://doi.org/10.30574/wjarr.2023.17.1.0070

Abstract

Lead-free perovskite gained much more attention of researchers in the field of electronics and photovoltaics due to the toxicity issue of the lead-based perovskite. Using first principle approach based on density functional theory (DFT), the electronic and optical properties of methylammonium tin halide (MTH) perovskite $ASnX_3$ ($A = CH_3NH_3$, X = Cl, Br, I) is calculated, the key material for optoelectronic applications, especially for solar cells. The halide contents control the electronic and optical characteristics of material such as orbitals, density of states and optical conductivity. We have identified orbitals consisting of valence and conduction band. Furthermore, the compound $ASnI_3$ shows a suitable band gap than all others compound which makes him suitable candidate for solar cells application.

Keywords: Perovskite; DFT; Solar cells; Optoelectronic

1. Introduction

Day-by-day energy demands increases with increase in population. The non-renewable energy sources like fossil fuels are limited in stock, costly and not environment friendly. So the researchers are attracted towards renewable energy resources which have low cost, eco-friendly and huge/unlimited stock. Currently, solar energy is one the most spreading renewable energy area in terms of market demand. Sun is the major source of energy and solar cells are used to take energy from sun and convert into electrical energy. The solar cells which are key material to convert sun energy into electrical energy, but are at high production and installation cost reduces its widespread use. Thus, efforts have been made to fabricate/find cheaper materials to replace silicon.

Recently, organic-inorganic perovskite gained popularity as alternate source of silicon due to low cost and high Power conversion efficiency (PCE) in solar cells [1-3]. The general chemical formula of organic-inorganic perovskite is AMX_3 where A stands for organic cation CH_3NH_3, M for metal ion (Pb, Sn) and X is halide (Cl, Br, I). The first reported PCE of perovskite solar cells was 3.8% reported by Kojima et al. [4] later using lead based perovskite $CH_3NH_3PbI_3$ the PCE approaches to 6.5% [5], 17.9% [6–8] then to over 22.7% [9–11]. The lead-based perovskite $CH_3NH_3PbX_3$ gained significant attention due to outstanding PCE as compared to silicon materials. The lead based perovskite can be applied in high temperature superconductors [12], optoelectronics (sensors, LEDs) [12, 13], electrodes [14], wearable electronics [15] and thermoelectric materials [16]. Recently we have investigated the optoelectronic properties of all lead based compounds using first principle approach [17], but the toxicity issue in lead-based perovskite reduces its use in commercializing in many applications [18, 19].

* Corresponding author: Wang Qun

The Tin-based perovskite has shown excellent mobility in transistors, which give him opportunity to explore in solar cells applications [20]. Both tin and lead belong to same group having similar valence configuration. As compared to lead the tin has exceptional properties like smaller effective mass of holes and narrow band gape which enhanced photon absorption. The previous study by Umari et al has shown that $CH_3NH_3SnI_3$ deliver high photocurrent density due to narrow band gap (E_g) as compared to $CH_3NH_3PbI_3$ [21]. Computational studies on structural, electronic and optical properties of Tin-based perovskite can gain insight into these important compounds.

In this work we have calculated the electronic and optical properties of Tin-based perovskite, methylammonium tin halide (MTH) $ASnX_3$ where (A=CH_3NH_3, X=Cl, Br, I) using first principle approach. In the electronic study, band structures, density of states and in optical study, the absorption coefficient, optical conductivity, refractive index, reflectivity and dielectric constant are analyzed.

2. Material and methods

In present calculations, we used Wien2k software based on density functional theory (DFT). The structure optimization is done using generalized gradient approximation (GGA) [22-25]. The calculations of MTHs was carried out with 'Full potential linearized augmented plane wave (FP-LAPW) approach implemented in Wien2k code. The radii of muffin-tin sphere for MTHs are $1.31a_0$, $0.68a_0$, $1.27a_0$ for C, H and N respectively while $2.5a_0$ for Sn, Cl, Br and I. The self-consistent field cycle (SCF) calculations convergence is attained at 0.7 mR_y as well as the convergence of charge 0.0001e. All the MTH compounds are in simple cubic structure, we make a super cell of (2 x 2 x 1) of every structure. The lattice constants all compounds in present calculations are optimized and relaxed the structure (atomic positions) till forces convergence becomes ($5x10^{-3}$ eV/A°) and energy value becomes 10^{-4} eV. In present calculations for better convergence of charge in DMS, the wave cut-off value $R_{mt}K_{max}$ = 8 in interstitial region, 2000 k-points and Gmax = 20 is taken.

3. Results and discussion

3.1. Band structures

The MTH perovskite compounds adopt cubic crystal structures at high temperature with semiconductor and semi-metal like behavior.[26-29] The structure is constructed of a network SnX_6 (X= Cl, I, Br) corner shared octahedral contain organic cation CH_3NH_3. The organic cation is free to rotate at high temperature because organic cation does not form a strong bond with halide atoms. [30, 31] The fig 1(a) shows crystal structure of $ASnX_3$ compounds which contain Sn at the center of unit cell, halides contents (Cl, Br, I) at sides and CH_3NH_3 at corners. We have optimized lattice constants and relaxed atomic positions, the lattice constants (a=b=c) $CH_3NH_3SnCl_3$, $CH_3NH_3SnBr_3$ and $CH_3NH_3SnI_3$ are 6.29 Å, 5.96 Å and 6.32 Å respectively which shows good agreement with previous experimental and theoretical findings [28, 32].

The brillouin zone of simple cubic structure of $ASnX_3$ is shown in fig 1(b) [33], we draw all the all the K points of simple cubic structure of ASnX3 from point Γ to Γ in Γ R X M Γ manner in side cubic brillouin zone.

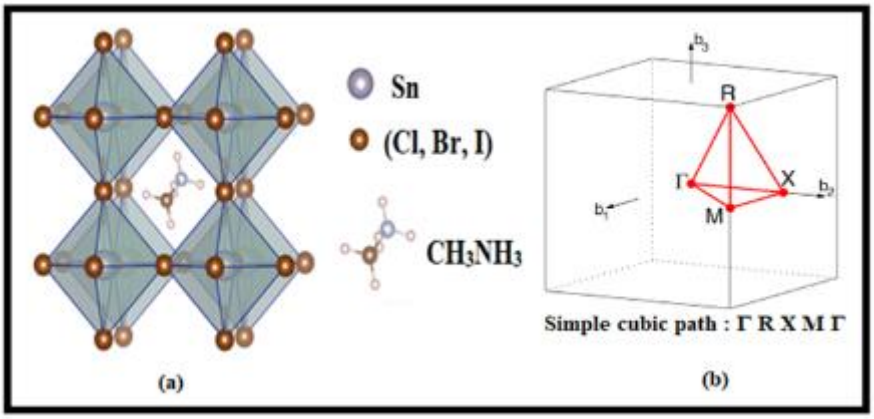

Figure 1 (a) The Crystal structure of $ASnX_3$ and (b) simple cubic brillouin zone (path)

To describe electronic properties we have plotted band structures and density of states and absorption coefficient, reflectivity, dielectric constant, refractive index and optical conductivity for optical properties using Xmgrace software in Wien2k.

The compounds $ASnCl_3$ shows semi-metallic like behavior due to spontaneous hole carrier doping because of oxidation of Sn^{2+} to Sn^{4+} [26, 27]. All results clarify good agreements with previous theoretical and experimental findings [34, 35]. In fig 2, the band structures of $ASnX_3$ shows the band gape at R and M points. The band gap of $ASnBr_3$ is E_g=1.67 eV which is direct bang gap shown in fig 2(b). The conduction band minima and valence band maxima occurred at point M in case of $ASnBr_3$ band structures. Also, the $ASnI_3$ compound band gap is found to be direct (E_g= 1.34 eV) which occurs at point R shown in fig 2(c).

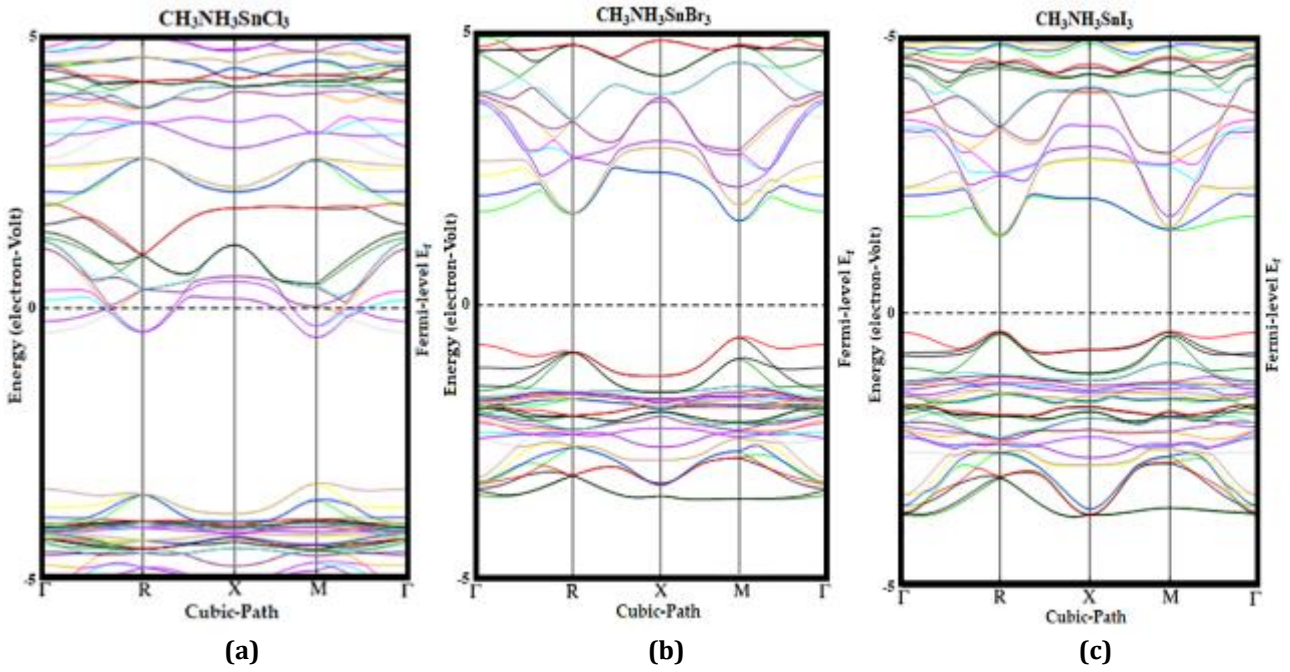

Figure 2 Band structure calculations of (a) $ASnCl_3$, (b) $ASnBr_3$ and (c) $ASnI_3$

3.2. Density of states

To discuss more about band structure the density of states information is very helpful. The total and partial densities of states are plotted for $ASnX_3$ compounds shown in fig 3. For $ASnX_3$ all compound total density of states (TDOS) described that the main contribution at the valence band (VB) edges towards conduction band (CB) and Conduction band edges towards valence band is due to p-orbital of Sn and halide contents (Cl, Br, I).

For $ASnCl_3$ TDOS shown if fig 3(a), the major contribution is noted in VB due to Cl-p orbital and Sn P orbital and minor contribution of N-p orbital is detected. Looking towards CB the major contribution towards VB edges is due to Sn-p and Cl-p orbitals while minor contribution is detected of N-p orbital. The partial density of states (PDOS) of $ASnCl_3$ shown in fig 3(b), reveals the fact that, main contribution at VB towards CB edges is due to Cl-p_x, Cl-p_y and minor contribution of Sn-p_z. Additionally, inside CB the Sn-p_x, Sn-p_y, Sn-p_z and Cl-p_z are dominant.

For $ASnBr_3$ TDOS shown in fig 4(a), the main contribution towards CB and VB (both edges) is due to Br-p and Sn-p orbitals while minor contribution of N-p orbital is detected. For $ASnBr_3$ PDOS shown in fig 4(b), the major and minor contribution in VB is due to Br-p_x, Br-p_y, Br-p_z, Sn-p_y and Sn-p and N-p_x respectively. At CB the major contribution of Sn-p_x, Sn-p_y, Sn-p_z and Br-p_x and minor contribution of N-p_x is detected.

For $ASnI_3$ TDOS shown in fig 5(a), the major contribution in VB and CB towards edges and is due to Sn-p and I-p orbitals while minor contribution of N-p orbitals is detected. Moreover, the PDOS of $ASnI_3$ shown in fig 5(b), major contribution in VB edges is due to I-p_x, I-p_y and I-p_z while in CB Sn-p_x, Sn-p_y and Sn-p_z contribution is dominant. Throughout whole study, it is noted that the halide contribution is dominant in VB and Sn contribution is dominant in CB. The narrow band gap E_g as compared to lead makes these compounds very effective in optoelectronic industry [25].

Table 1 Structural parameters of $ASnX_3$

MTH	Crystal structure	Bond length (A°)	Lattice constant (A°)
$ASnCl_3$	Cubic	C-H=1.860, N-H=1.030, Sn-C=4.955 Sn-I=3.121, N-Pb=4.820	a = b = c = 6.29
$ASnBr_3$	Cubic	C-H=1.097, N-H=1.039, Sn-C=4.729 Sn-Br=2.960, N-Pb=4.555	a = b = c = 5.96
$ASnI_3$	Cubic	C-H=1.095, N-H=1.039, Sn-C=4.7624 Sn-Br=2.859, N-Pb=4.317	a = b = c = 6.32

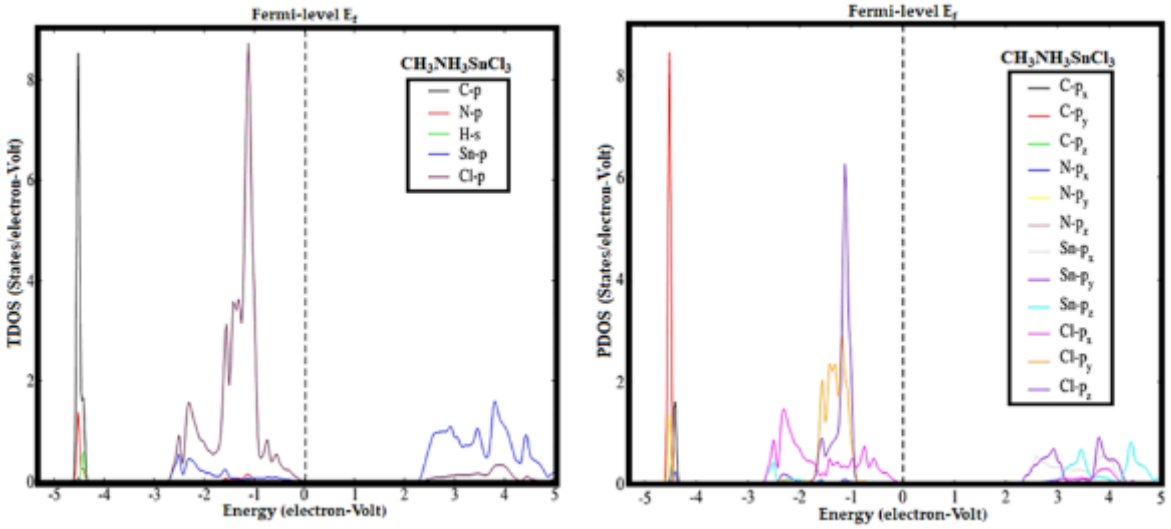

(a) (b)

Figure 3 Total density of states (a) and Partial density of states (b) of $ASnCl_3$

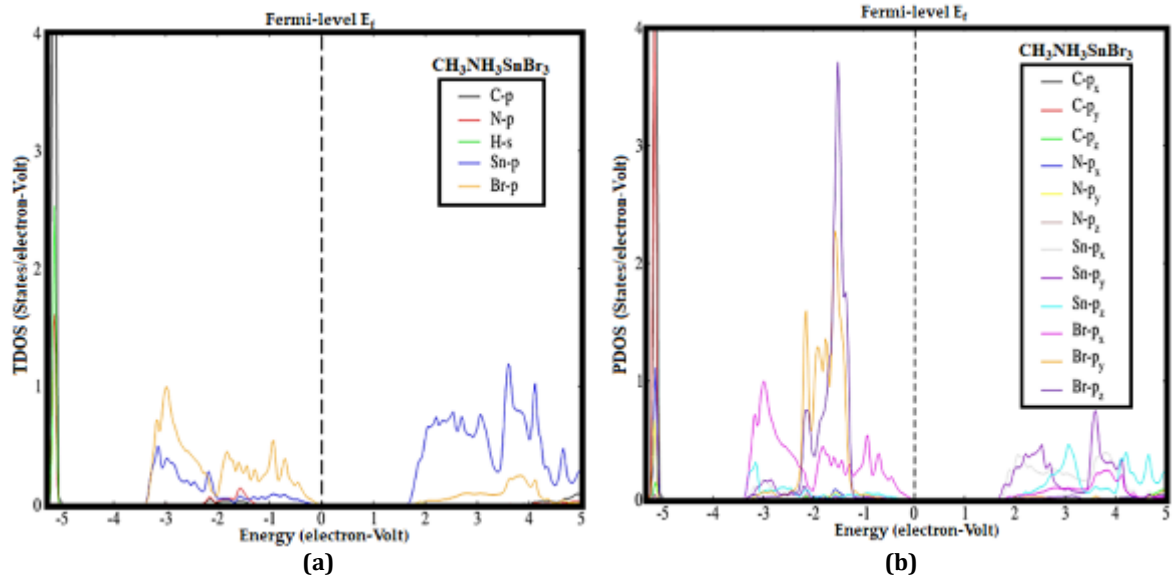

(a) **(b)**

Figure 4 Total density of states (a) and Partial density of states (b) of $ASnBr_3$

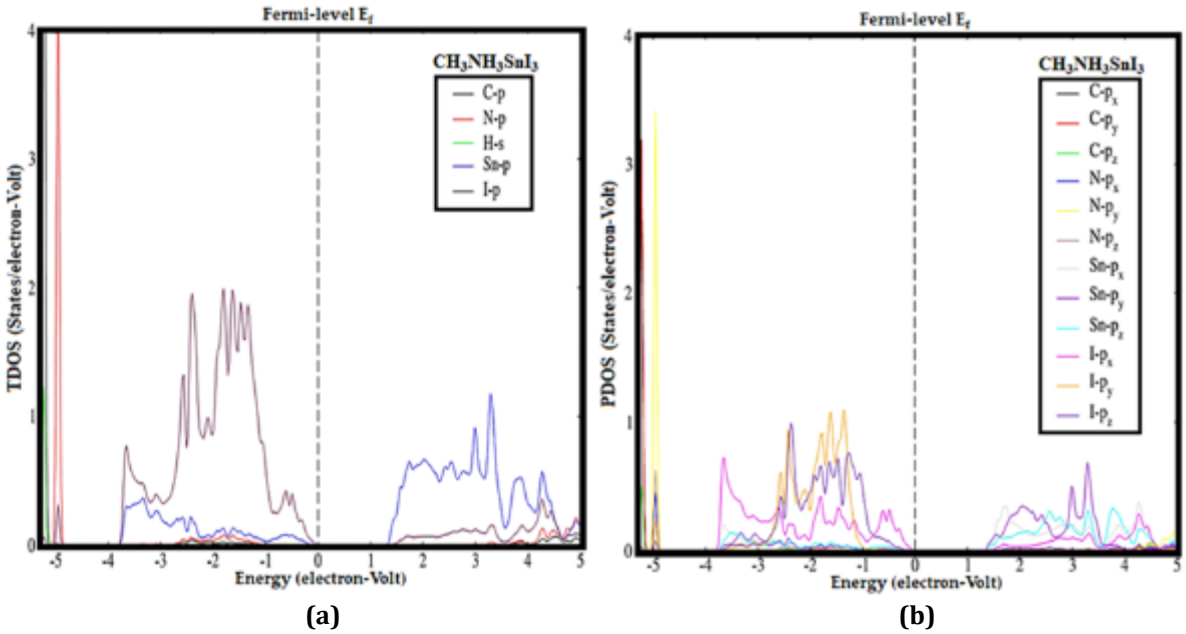

Figure 5 Total density of states (a) and Partial density of states (b) of ASnI3

Table 2 Measured electronic gapes Eg of ASnX3 using Generalized gradient approximation (GGA)

MTH	Computational Method	Electronic band gap E_g
$ASnCl_3$	GGA	Metallic
$ASnBr_3$	GGA	1.67 eV
$ASnI_3$	GGA	1.34 eV

3.3. Optical properties

The optical properties can be define as ''the interaction of electromagnetic (EM) radiations with matter in visible''. The electromagnetic radiation spectrum consists of different ranges of wavelengths starting from harmful gamma rays and ending on radio waves. The visible range is in between 0.390 to 0.770 μm, which is very important for studying many optical parameters.

The absorption coefficient α (ω) is a measurement looking at how far beam of light (different wavelengths) can go through material before it gets absorbed. The material absorption coefficient is depends on material thinness, if it is so thin then the light beam will be

$$\alpha(\omega) = -\frac{\ln(1-A)}{x} \qquad (3.1)$$

Where α (ω) indicates absorption coefficient, A is percentage of light absorbed and x is thickness of material. For percentage of light absorption A and for thickness x, equation 3.1 can be written as

$$A = 1 - e^{-\alpha x} \qquad (3.2)$$

$$x = -\frac{\ln(1-A)}{\alpha(\omega)} \qquad (3.3)$$

The absorption coefficient determines how much penetration occurs of certain wavelength of light before it absorbed. Light is poorly absorbed in Material with low absorption co-efficient and if material is thin enough then it becomes transparent to that specific wavelength.

The absorption lines in fig 6(a) represent different compounds absorption in specific energy from (0-10eV) and shows that green line $ASnI_3$ has good absorption coefficient in desirable energy regime so it can absorb light as much than others. The compound $ASnI_3$ can absorb maximum wavelengths of light in visible region and first maximum peak occurs in that visible region. After $ASnI_3$ compound $ASnBr_3$ can absorbs light in visible region and increasing when energy increasing. The compound $ASnCl_3$ shows poor absorbance as compared to $ASnBr_3$ and $ASnI_3$. The $ASnI_3$ can be used as absorber inside solar cells due to its outstanding absorbance at visible energy.

The reflectivity $R(\omega)$ is ratio of reflected radiation flux Φ_r by surface to incident radiation flux Φ_i.

$$R(\omega) = \frac{\Phi_r}{\Phi_i} \qquad (3.4)$$

We have calculated the reflectivity of all ASnX3 compounds using GGA scheme as shown in fig 6(b). The black, red and green lines represent the behavior of compounds ASnCl3, ASnBr3 and ASnI3 respectively. One can see objects by reflection clearly. The first maximum peak is noted for ASnI3 at energy of 2.2 eV.

The dielectric constant of ASnX3 is calculated using GGA scheme. The two parts of dielectric constant, real part $\varepsilon 1\ (\omega)$ and imaginary part $\varepsilon 2\ (\omega)$ represent charge polarization and dissipation respectively shown in fig 7(a) & (b). The higher dielectric constant is founded for $ASnI_3$ as compared to other compounds. The black, red and green lines indicate compounds $ASnCl_3$, ASnBr3 and $ASnI_3$ respectively. While discussing imaginary part the $ASnX_3$ is reported for maximum wave damping because it is semiconductor in nature. So a high dielectric constant reduces exciton binding energy, which reduces charge carrier losses and enhances the performance of solar cell.

In optics refractive index n is dimensionless number that describes the light propagation in medium. Mathematically it can be expressed as

$$n = \frac{c}{v} \qquad (3.5)$$

Where c speed of light in vacuum and v is phase velocity in medium. The two parts of refractive index is calculated, the real part $n_1(\omega)$ and imaginary part $n_2(\omega)$ using GGA scheme. The real parts represent speed of light ratio while imaginary indicates absorption. In both parts the compound $ASnI_3$ is dominant. The $ASnI_3$ has good refractive index in visible energy limit and also is absorb more energy than others. The fig 8(a) & (b) shows real and imaginary part of refractive index.

Optical conductivity is the property of material, which produces charge conduction when it placed under electromagnetic radiations. The optical conductivity is material property, which relates current density to to electric field. Mathematically it can be written as

$$J(\omega) = \sigma(\omega)\mathrm{E}(\omega) \qquad (3.6)$$

In eq (3.6) $J(\omega)$ is current density vector, $\sigma(\omega)$ is optical conductivity and $\mathrm{E}(\omega)$ represent electric field vector.

The optical conductivity $\sigma(\omega)$ of $ASnX_3$ describes the behavior of these compounds in presence of energy (eV). Within the visible energy range (1.63-3.26eV) the compound $ASnI_3$ shows outstanding behavior as compared to other. So the compound $ASnI_3$ can be used as good candidate in optoelectronic industry especially in solar cells. The optical conductivity $\sigma(\omega)$ is illustrated in fig 9 against energy in electron-volt (eV).

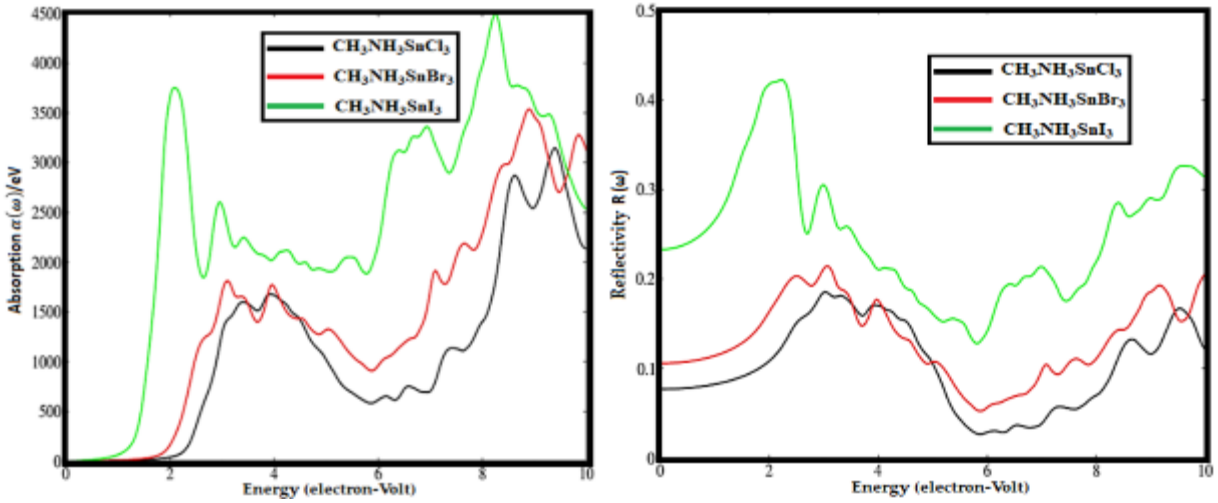

(a) (b)

Figure 6 Optical properties of $ASnX_3$ (a) Absorption cofficeint and (b) Refelectivity

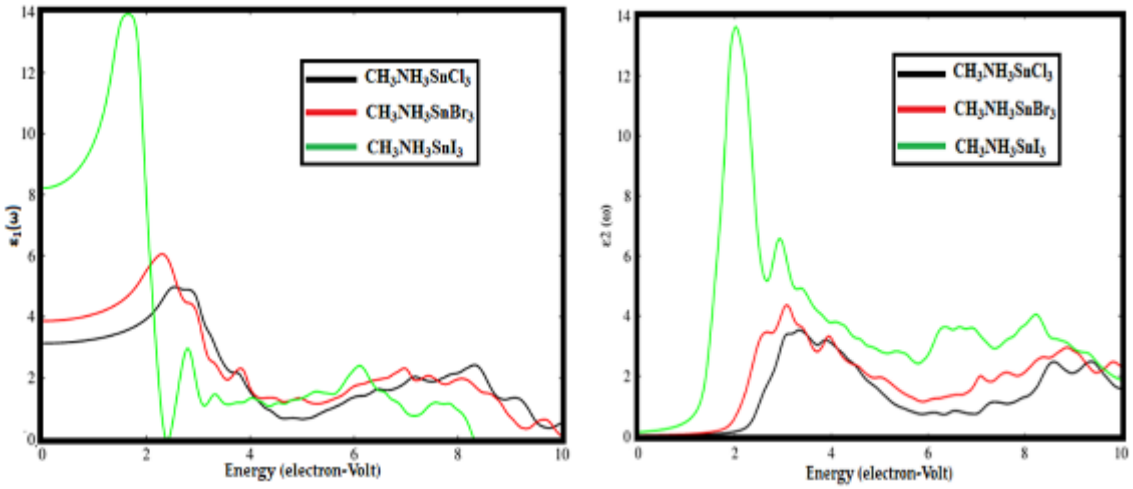

(a) (b)

Figure 7 Optical properties of $ASnX_3$ (a) Real part of dielectric constant and (b) Imaginary part of dielectric constant

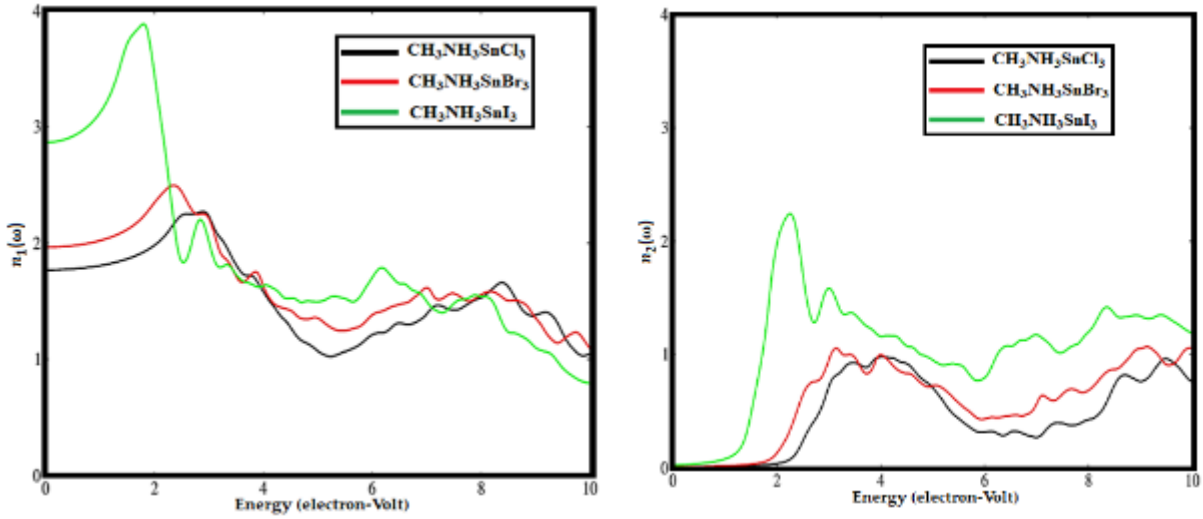

(a) (b)

Figure 8 Optical properties of $ASnX_3$ (a) Real part of refractive index and (b) Imaginary part of refractive index

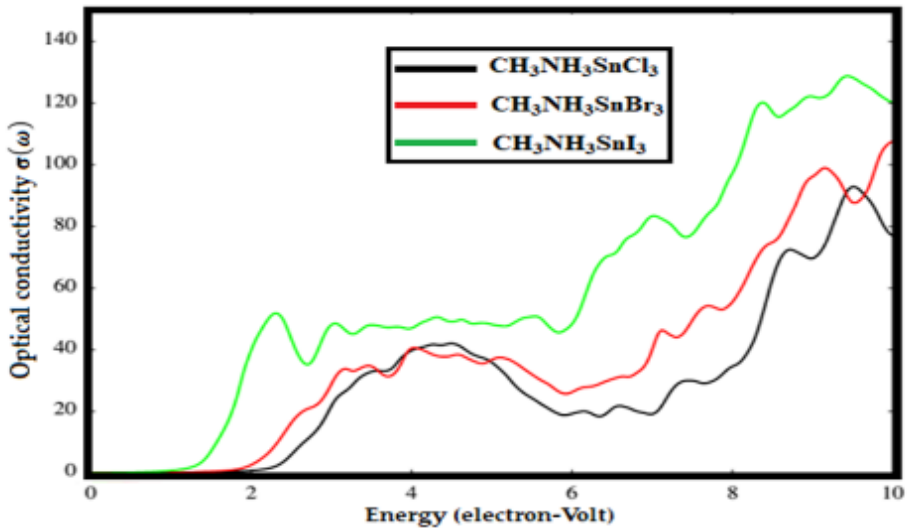

Figure 9 Optical conductivity of $ASnX_3$

Table 3 Measured values Absorption coefficient and optical conductivity using GGA

MTH	Absorption		Optical conductivity	
	α (ω)	E (eV)	σ (ω)	E (eV)
$ASnCl_3$	2873	8.635	92.850	9.518
$ASnBr_3$	3535	8.910	98.890	9.162
$ASnI_3$	4498	8.280	128.555	9.430

4. Conclusion

In summary, we have calculated the electronic and optical properties of MTH perovskite $ASnX_3$ where, ($A=CH_3NH_3$, X=Cl, Br, I) using first principles approach. Our calculated band gapes nearly agrees with prvious experimental and theoratical findings. The p orbital of halide contents (Cl, Br, I) atom governs Valence band and conduction band mostly consist of p orbital of Sn atom. The iodide based compound $ASnI_3$ shows narrow band gape (Eg=1.35eV) which can transferred more electron then others. The optical properties of $ASnX_3$ is calcuated and graphs are plotted against enegy (eV). The optical conductivity and absorption coeffieceint of $ASnI_3$ is outstanding behavior in desirable energy limit, so the compound $ASnI_3$ is more suitable candidate for optoelectronic industry.

Compliance with ethical standards

Acknowledgments

I am very much thankful for Co-author Waqas Khan for technical and financial support to publish this article. Eng. Dr. Murtaza khan for layout, Yasar ali for technical writing, fazal dayan for calculations support and AL-GALAL HASAN MUNASSAR SALEH for analyzing data and plotting. Without you all it was impossible to publish such complicated task. Again Special thanks to Waqas khan for funding and technical writing of manuscript without demanding any favors. I will remember you for such nice actions throughout my research life.

Disclosure of conflict of interest

The authors declare no conflict of interest.

References

[1] Candan A, Kurban M. Electronic structure, elastic and phonon properties of perovskite-type hydrides MgXH3 (X= Fe, Co) for hydrogen storage. Solid State Communications. 2018 Oct 1;281:38-43.

[2] Kurban M, Kürkçü C, Yamçıçıer Ç, Göktaş F. A study of structural phase transitions and optoelectronic properties of perovskite-type hydride MgFeH3: ab initio calculations. Journal of Physics: Condensed Matter. 2019 May 14;31(30):305401.

[3] Tai Q, Tang KC, Yan F. Recent progress of inorganic perovskite solar cells. Energy & Environmental Science. 2019;12(8):2375-405.

[4] Kojima A, Teshima K, Shirai Y, Miyasaka T. Organometal halide perovskites as visible-light sensitizers for photovoltaic cells. Journal of the american chemical society. 2009 May 6;131(17):6050-1.

[5] Im JH, Lee CR, Lee JW, Park SW, Park NG. 6.5% efficient perovskite quantum-dot-sensitized solar cell. Nanoscale. 2011;3(10):4088-93.

[6] Noel NK, Stranks SD, Abate A, Wehrenfennig C, Guarnera S, Haghighirad AA, Sadhanala A, Eperon GE, Pathak SK, Johnston MB, Petrozza A. Lead-free organic–inorganic tin halide perovskites for photovoltaic applications. Energy & Environmental Science. 2014;7(9):3061-8.

[7] Lee MM, Teuscher J, Miyasaka T, Murakami TN, Snaith HJ. Efficient hybrid solar cells based on meso-superstructured organometal halide perovskites. Science. 2012 Nov 2;338(6107):643-7.

[8] Noh JH, Im SH, Heo JH, Mandal TN, Seok SI. Chemical management for colorful, efficient, and stable inorganic–organic hybrid nanostructured solar cells. Nano letters. 2013 Apr 10;13(4):1764-9.

[9] Hoefler SF, Trimmel G, Rath T. Progress on lead-free metal halide perovskites for photovoltaic applications: a review. Monatshefte für Chemie-Chemical Monthly. 2017 May;148(5):795-826.

[10] Jiang F, Yang D, Jiang Y, Liu T, Zhao X, Ming Y, Luo B, Qin F, Fan J, Han H, Zhang L. Chlorine-incorporation-induced formation of the layered phase for antimony-based lead-free perovskite solar cells. Journal of the American Chemical Society. 2018 Jan 24;140(3):1019-27.

[11] Ono LK, Qi Y. Research progress on organic–inorganic halide perovskite materials and solar cells. Journal of Physics D: Applied Physics. 2018 Feb 9;51(9):093001.

[12] Frohna K, Stranks SD. Hybrid perovskites for device applications. InHandbook of Organic Materials for Electronic and Photonic Devices 2019 Jan 1 (pp. 211-256). Woodhead Publishing.

[13] Khandy SA, Gupta DC. Structural, elastic and thermo-electronic properties of paramagnetic perovskite PbTaO3. RSC advances. 2016;6(53):48009-15.

[14] Khandy SA, Gupta DC. Investigation of structural, magneto-electronic, and thermoelectric response of ductile SnAlO3 from high-throughput DFT calculations. International Journal of Quantum Chemistry. 2017 Apr 15;117(8):e25351.

[15] Shi B, Duan L, Zhao Y, Luo J, Zhang X. Semitransparent perovskite solar cells: from materials and devices to applications. Advanced Materials. 2020 Jan;32(3):1806474.

[16] Khandy SA, Gupta DC. Electronic structure, magnetism and thermoelectricity in layered perovskites: Sr2SnMnO6 and Sr2SnFeO6. Journal of Magnetism and Magnetic Materials. 2017 Nov 1;441:166-73.

[17] Jin X, Wang Q, Jadoon AM. Opto-Electronic Properties of Methyl-Ammonium Lead Halide: A First Principle Approach. In Journal of Physics: Conference Series 2020 Sep 1 (Vol. 1622, No. 1, p. 012105). IOP Publishing.

[18] Jiang F, Yang D, Jiang Y, Liu T, Zhao X, Ming Y, Luo B, Qin F, Fan J, Han H, Zhang L. Chlorine-incorporation-induced formation of the layered phase for antimony-based lead-free perovskite solar cells. Journal of the American Chemical Society. 2018 Jan 24;140(3):1019-27.

[19] Zhao XG, Yang JH, Fu Y, Yang D, Xu Q, Yu L, Wei SH, Zhang L. Design of lead-free inorganic halide perovskites for solar cells via cation-transmutation. Journal of the American Chemical Society. 2017 Feb 22;139(7):2630-8.

[20] Kagan CR, Mitzi DB, Dimitrakopoulos CD. Organic-inorganic hybrid materials as semiconducting channels in thin-film field-effect transistors. Science. 1999 Oct 29;286(5441):945-7.

[21] Umari P, Mosconi E, De Angelis F. Relativistic GW calculations on CH3NH3PbI3 and CH3NH3SnI3 perovskites for solar cell applications. Scientific reports. 2014 Mar 26;4(1):1-7.

[22] Perdew JP. Density-functional approximation for the correlation energy of the inhomogeneous electron gas. Physical Review B. 1986 Jun 15;33(12):8822.

[23] Schwarz K. DFT calculations of solids with LAPW and WIEN2k. Journal of Solid State Chemistry. 2003 Dec 1;176(2):319-28.

[24] Schwarz K, Blaha P, Trickey SB. Electronic structure of solids with WIEN2k. Molecular Physics. 2010 Nov 10;108(21-23):3147-66.

[25] Slater JC. Introduction to chemical physics. Read Books Ltd; 2011 Mar 23.

[26] Takahashi Y, Obara R, Lin ZZ, Takahashi Y, Naito T, Inabe T, Ishibashi S, Terakura K. Charge-transport in tin-iodide perovskite CH 3 NH 3 SnI 3: origin of high conductivity. Dalton Transactions. 2011;40(20):5563-8.

[27] Stoumpos CC, Kanatzidis MG. The renaissance of halide perovskites and their evolution as emerging semiconductors. Accounts of chemical research. 2015 Oct 20;48(10):2791-802.

[28] Chiarella F, Zappettini A, Licci F, Borriello I, Cantele G, Ninno D, Cassinese A, Vaglio R. Combined experimental and theoretical investigation of optical, structural, and electronic properties of C H 3 N H 3 Sn X3 thin films (X= Cl, Br). Physical Review B. 2008 Jan 25;77(4):045129.

[29] Borriello I, Cantele G, Ninno D. Ab initio investigation of hybrid organic-inorganic perovskites based on tin halides. Physical Review B. 2008 Jun 23;77(23):235214.

[30] Chang YH, Park CH, Matsuishi K. First-principles study of the Structural and the electronic properties of the lead-Halide-based inorganic-organic perovskites (CH3NH3) PbX3 and CsPbX3 (X= Cl, Br, I). Journal-Korean Physical Society. 2004 Apr 1;44:889-93.

[31] Wasylishen RE, Knop O, Macdonald JB. Cation rotation in methylammonium lead halides. Solid state communications. 1985 Nov 1;56(7):581-2.

[32] Setyawan W, Curtarolo S. High-throughput electronic band structure calculations: Challenges and tools. Computational materials science. 2010 Aug 1;49(2):299-312.

[33] Takahashi Y, Obara R, Lin ZZ, Takahashi Y, Naito T, Inabe T, Ishibashi S, Terakura K. Charge-transport in tin-iodide perovskite CH3NH3SnI3: origin of high conductivity. Dalton Transactions. 2011;40(20):5563-8.

[34] Bernal C, Yang K. First-principles hybrid functional study of the organic–inorganic perovskites CH3NH3SnBr3 and CH3NH3SnI3. The Journal of Physical Chemistry C. 2014 Oct 23;118(42):24383-8.

[35] Hao F, Stoumpos CC, Cao DH, Chang RP, Kanatzidis MG. Lead-free solid-state organic–inorganic halide perovskite solar cells. Nature photonics. 2014 Jun;8(6):489-94.

Author's short biography

Dr. Mehtab Ur Rehman Sahir, has done his BS and MS in Physics and Master in education from Pakistan. After he joined Beijing University of technology, China to obtain PhD in material science & engineering. His expertise's are Physical vapour deposition PVD, Physical metallurgy, solid state manufacturing material and first principle. Dr. Mehtab-Ur-Rehman Sahir has many of research papers in the area of theoretical physiscs, solar cells architecture, thin films and experimental Material science.